Transactions on Environment, Energy and Earth Sciences
ISSN: 2960-1924, eISSN: 2960-2300 | Volume 4
GEMFE 2024

Immersion Phased Array Ultrasonic Inspection for Aluminum Liner of Carbon Fibre Composite Overwrapped Pressure Vessel

Yangji Tao, Zhongqiang Liu *, Ping Tang, Cunjian Miao, Guoyang Teng, Yan Shi

Zhejiang Academy of Special Equipment Science, Key Laboratory of Special Equipment Safety Testing Technology of Zhejiang Province, Hangzhou, China

* Corresponding Author Email: zjulzq@126.com

Abstract. Carbon fibre composite overwrapped pressure vessels (type Ⅲ pressure vessels for short) are widely used in hydrogen fuel cell vehicles. The aluminum liner of type Ⅲ pressure vessels bearing the hydrogen pressure and fiber tension simultaneously requires factory inspections. It is difficult to detect the aluminum liner with different curvature by the phased array ultrasonic testing. An aluminum liner detection method was proposed based on the immersion phased array ultrasonic testing. The thickness of the aluminum liner was measured by avoiding overlapping reflected waves. Besides, the longitudinal defects were detected by the circumferential shear wave scanning, and transverse defects were detected by the bidirectional deflecting scanning. The above three modes were verified by the acoustic field simulation and inspection simulation using CIVA. Results show that the proposed detection method is highly reliable for the thickness measurement and defect detection of the aluminum liner.

Keywords: Aluminum liner; immersion phased array ultrasonic testing; thickness measurement; circumferential shear wave scanning; bidirectional deflecting scanning.

1. Introduction

Hydrogen can be stored under compressed form at pressures ranging from 20 MPa to 100 MPa in pressure vessels [1, 2]. Hydrogen storage vessels have four main types. Currently, type III pressure vessels are widely used in hydrogen fuel cell vehicles for their light weight, high pressure, large capacity [3-5]. Type III pressure vessels are made of a metallic liner overwrapped with carbon fibre composite [6, 7]. The inner metallic liner is a seamless aluminum liner manufactured by drawing and forming of tubes. The aluminum liner is exposed to hydrogen, without hydrogen embrittlement and hydrogen permeation. Besides, the carbon fibre composite is carbon fibres embedded in a polymer matrix. Type III pressure vessels are under cyclic loading, due to frequent charging and discharging in operation. The aluminum liner bears the hydrogen pressure and fiber tension simultaneously. Therefore, the factory inspection of the aluminum liner is essential to ensure the pressure vessel infrastructure.

Ultrasonic testing (UT) is one of the most common inspection methods used to detect flaws. Phased array ultrasonic testing (PAUT) has greater inspecting performance, which realizes the beam focusing and deflecting by adjusting the phase delay. The PAUT technology has been utilized to inspect multi-layered steel vessels and welded steel pipes [8-10]. In their studies, the probe with a special shape wedge was used to inspect curved parts. However, the fixed shape of the wedge or probe is hard to detect aluminum liners of different diameters and different parts of an aluminum liner.

Immersion phased array ultrasonic testing (IPAUT) has been selected to inspect aluminum liners for the advantages of high versatility and high repeatability [11-13]. The IPAUT has high versatility because it can adapt to complex-shaped vessels regardless of the inspected vessel's shape and size. Moreover, the IPAUT has high repeatability because it can get the same measurements under identical conditions using water as a coupling medium.

In this study, we proposed an aluminum liner detection method to inspect the aluminum liner of type III pressure vessels based on the IPAUT. The thicknesses of different parts in the aluminum liner were measured by avoiding overlapping reflected waves. In addition, the longitudinal defects were detected by the circumferential shear wave scanning, and transverse defects were detected by the bidirectional deflecting scanning. The above three modes were verified by the acoustic field simulation and inspection simulation using CIVA.

2. Aluminum Liner Detection Method

The aluminum liner of type III pressure vessels was selected as the inspection object. A typical aluminum liner consisted of a cylindrical main body enclosed by two ellipsoidal dome heads, as shown in Fig.1. Aluminum liners of different diameters and different parts of the aluminum liner had different curvature.

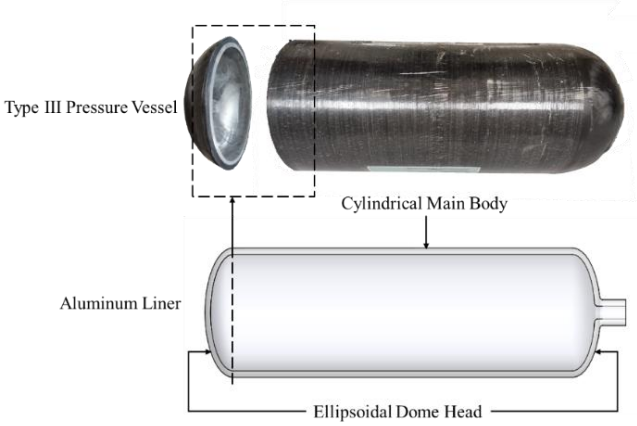

Figure 1. The type III pressure vessel and the aluminum liner

The IPAUT was advantageous for the inspection of curved surfaces because the ultrasonic phased array probe did not directly contact the aluminum liner. An aluminum liner detection method was proposed to inspect the aluminum liner based on the IPAUT, as shown in Fig.2. The aluminum liner rotated around the center of the circle, and the probe scanned along the cross-sectional of the aluminum liner. By rotating the probe, the angle of incidence of the probe could be adjusted to fit the surface profile of aluminum liners.

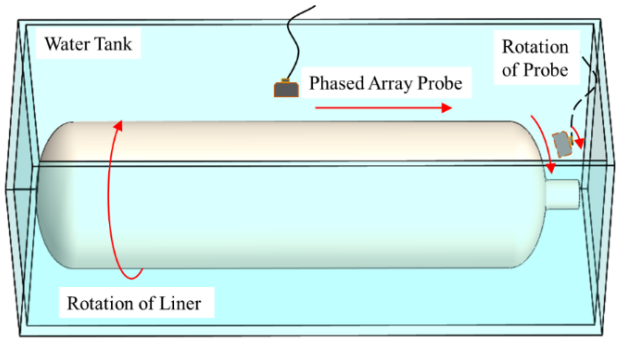

Figure 2. The aluminum liner detection method

The aluminum liner detection method included the thickness measurement and defect detection. There were two main types of defects in the aluminum liner, namely the longitudinal defect and transverse defect. The longitudinal defects were detected by the circumferential shear wave scanning, and transverse defects were detected by the bidirectional deflecting scanning.

2.1. Thickness Measurement

Thickness measurement is essential for the aluminum liner detection method because the liner thickness influences the load-bearing capacity. The IPAUT uses water as a coupling medium. In order

to reach the aluminum liner, the ultrasonic wave from the ultrasonic phased array probe needs to pass through the water layer. The transmission of ultrasonic waves is shown in Fig. 3. At the interface between the water layer and the aluminum liner, part of the ultrasonic wave enters the aluminum liner, and the rest is reflected back into water and received by the probe. Then, the incident wave entering the aluminum liner also is reflected into water and received by the probe, as it encounters the inner surface of the aluminum liner.

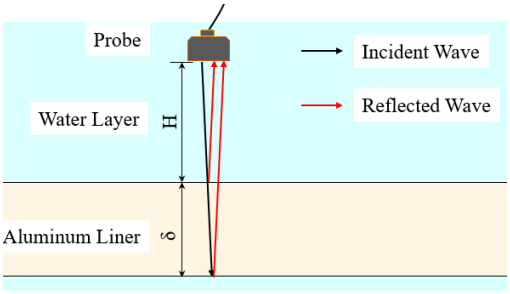

Figure 3. The transmission of ultrasonic waves in the thickness measurement

In the transmission of ultrasonic waves, there are incident and reflected waves at each interface. The reflected waves of the inner surface may overlap with those of the water layer so that they cannot be distinguished. To distinguish reflected waves, the thickness of the water layer is calculated by (1). The second reflected wave of the water layer overlaps with the fourth reflected wave of the inner surface. The first three reflected waves of the inner surface can be clearly distinguished.

$$H = 4 * \delta * c_{L\text{-}water}/c_{L\text{-}Al} \quad (1)$$

Where

H is the thickness of the water layer,

δ is the thickness of the aluminum liner,

$c_{L\text{-}water}$ is the velocity of longitudinal wave in water,

$c_{L\text{-}Al}$ is the velocity of longitudinal wave in aluminum.

2.2. Circumferential Shear Wave Scanning

In the circumferential shear wave scanning, the phase array probe is off-center of the aluminum liner, as shown in Fig. 4. The ultrasonic wave from the probe reaches the external surface of the aluminum liner with an incidence angle. There are longitudinal and shear waves with different angles of refracted waves, due to the different velocities of longitudinal and shear waves in aluminum. In order to get a single wave, we choose an incident angle between the first critical angle and the second critical angle. The shear wave will appear in the aluminum liner, but the longitudinal wave will not.

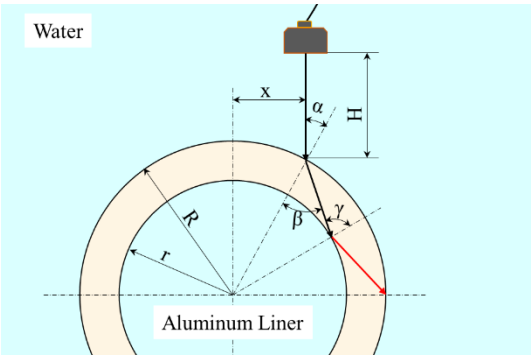

Figure 4. The transmission of ultrasonic waves in the circumferential shear wave scanning

The incident angle is calculated from the eccentricity and is greater than the first critical angle, as shown in (2).

$$\sin\alpha = \frac{x}{R} \geq \frac{c_{L-water}}{c_{L-Al}} \tag{2}$$

Where

α is the incident angle on the external surface of the aluminum liner,

x is the eccentricity of the probe,

R is the external radius of the aluminum liner.

The refracted shear wave needs to reach the inner surface of the aluminum liner. The incidence angle of the inner surface is less than 90 degrees. The incidence angle of 90 degrees is a critical state that the refracted shear wave is tangent to the inner surface. The refracted angle is associated with the incident angles of two surfaces, as shown in (3).

$$\sin\beta = \sin\alpha \cdot \frac{c_{S-Al}}{c_{L-water}} = \frac{x}{R} \cdot \frac{c_{S-Al}}{c_{L-water}} \leq \frac{r}{R} \tag{3}$$

Where

β is the refracted angle on the external surface of the aluminum liner,

r is the inner radius of the aluminum liner,

$c_{S\text{-}Al}$ is the velocity of shear wave in aluminum.

The eccentricity of the probe is adjusted in a range, as shown in (4).

$$R \cdot \frac{c_{L-water}}{c_{L-Al}} \leq x \leq r \cdot \frac{c_{L-water}}{c_{S-Al}} \tag{4}$$

2.3. Bidirectional deflecting Scanning

In the bidirectional deflecting scanning, the phase array probe emits ultrasonic waves in two directions, as shown in Fig. 5. The scanning in two directions is carried out simultaneously to enlarge the coverage area of scanning and improve detection efficiency.

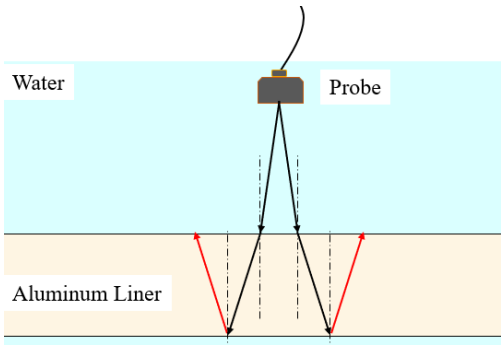

Figure 5. The transmission of ultrasonic waves in the bidirectional deflecting scanning

3. Simulation

The modes of thickness measurement and defect detection were verified by the acoustic field simulation using CIVA. Furthermore, the circumferential shear wave scanning and bidirectional deflecting scanning were also simulated in the inspection situation.

3.1. Acoustic Field Simulation

The acoustic fields for modes of the thickness measurement, circumferential shear wave scanning and bidirectional deflecting scanning are obtained, as shown in Fig.6. Fig.6 (a) and (b) show that the acoustic fields for the thickness measurement in the body and head are focusing on the inner surface of the aluminum liner. Fig.6 (c) shows that the shear wave acoustic field of the circumferential shear wave scanning is focusing on the external surface. Fig.6 (d) shows that the acoustic field of the bidirectional deflecting scanning covers twice the width of the phased array probe, focusing on the inner surface.

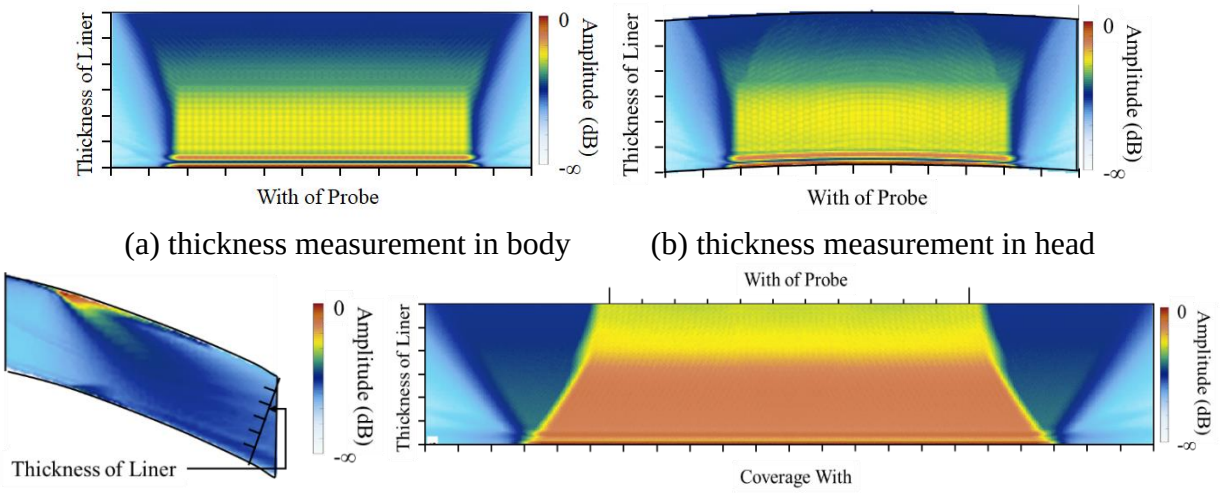

(a) thickness measurement in body (b) thickness measurement in head

(c) circumferential shear wave scanning (d) bidirectional deflecting scanning

Figure 6. The acoustic field simulation resluts

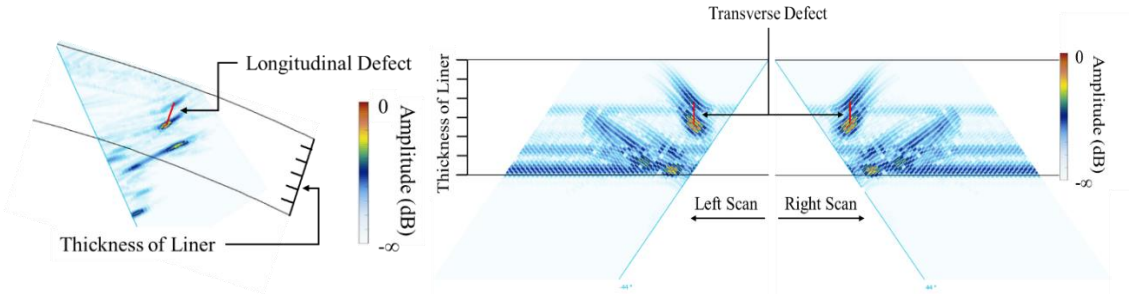

(a) longitudinal defect (b) transverse defect

Figure 7. The inspection simulation results

3.2. Inspection Simulation

The inspection simulation results for the longitudinal defect and transverse defect are obtained, as shown in Fig.7. Fig.7 (a) shows that a longitudinal defect is detected by the circumferential shear wave scanning. The defect signal consists of the reflected waves from the top and bottom of the longitudinal defect. The arrival time of two reflected waves can be used for accurate defect positioning and sizing. Fig.7 (b) shows that a transverse defect is detected by the bidirectional deflecting scanning. Because the transverse defect is just below the center of the probe, the results of the left scanning and right scanning are symmetrical. The transverse defect can also be accurately positioned and sized by reflected waves.

4. Conclusion

An aluminum liner detection method was proposed based on the IPAUT. In the thicknesses measurement, reflected waves were controlled without overlapping to clearly distinguish the inner surface. Besides, the longitudinal defects were detected by the circumferential shear wave scanning, and transverse defects were detected by the bidirectional deflecting scanning. The acoustic field simulation results showed that the proposed detection method was highly reliable for the thickness measurement and defect detection of the aluminum liner. The inspection simulation results showed that the longitudinal defect and transverse defect could be detected, positioned and sized.

Acknowledgments

This work was financially supported by the Science and Technology Program of the State Administration for Market Regulation (No. 2020MK045) and the Key R&D Program of Zhejiang Province (No. 2020C01118).

References

[1] H. Barthelemy, M. Weber, F. Barbier, "Hydrogen storage: Recent improvements and industrial perspectives," International Journal of Hydrogen Energy, vol. 42 (11), pp. 7254-7262, 2017.

[2] B.N. Nguyen, H.S. Roh, D.R. Merkel, et al, "A predictive modeling tool for damage analysis and design of hydrogen storage composite pressure vessels," International Journal of Hydrogen Energy, vol. 46 (39), pp. 20573-20585, 2021.

[3] D.J. Durbin, C. Malardier-Jugroot, "Review of hydrogen storage techniques for on board vehicle applications," International Journal of Hydrogen Energy, vol. 38 (34), pp. 14595-14617, 2013

[4] R.K. Ahluwalia, T.Q. Hua, J. K. Peng, et al, "Technical assessment of cryo-compressed hydrogen storage tank systems for automotive applications," International Journal of Hydrogen Energy, vol. 35 (9), pp. 4171-4184, 2010.

[5] J. Zheng, K. Ma, W. Zhou, et al, "High pressure hydrogen storage vessel for hydrogenation station, " Press Vessel Technol, vol. 35 (9), pp. 35-42, 2018.

[6] P.F. Liu, J.K. Chu, S.J. Hou, et al, "Numerical simulation and optimal design for composite high-pressure hydrogen storage vessel: A review," Renewable and Sustainable Energy Reviews, vol. 16 (4), pp. 1817-1827, 2012.

[7] P. Sharma, S. Sharma, T. Bera, et al. "Effects of dome shape on burst and weight performance of a type-3 composite pressure vessel for storage of compressed hydrogen," Composite Structures, vol. 293, pp. 115732, 2022.

[8] T. Yu, W. Guo, C. Miao, et al. "Study on inserted curved surface coupling phased array ultrasonic inspection of multi-layered steel vessel for high-pressure hydrogen storage," International Journal of Hydrogen Energy, vol. 46 (35), pp.18433-18444, 2021.

[9] C. Miao, Q. He, X. Du, et al. "The Phased Array Ultrasonic Inner Inspection for the Butt Weld on the Head of High-Pressure Vessel," Proceedings of the ASME 2018 Pressure Vessels and Piping Conference. Volume 5: High-Pressure Technology; ASME Nondestructive Evaluation, Diagnosis and Prognosis Division (NDPD); Rudy Scavuzzo Student Paper Symposium and 26th Annual Student Paper Competition. Prague, Czech Republic. July 15–20, 2018. V005T09A008.

[10] Y. Zhou, X. Qian, A. Birnie, et al. "A reference free ultrasonic phased array to identify surface cracks in welded steel pipes based on transmissibility," International Journal of Pressure Vessels and Piping, vol. 168, pp.66-78, 2018.

[11] S. Guan, X. Wang, L. Hua, et al. "Ultrasonic phased array inspection of aeroengine casing ring forgings using adaptive filtering and angle gain compensation algorithm," Applied Acoustics, vol. 195, pp. 108833, 2022.

[12] R. Wang, B. Li, B. Jiang, et al. "Automated immersion ultrasonic testing technology for debonding defects of the brazed joint of DOME in EAST divertor," Fusion Engineering and Design, vol. 176, pp. 113008, 2022.

[13] Q. Jiang, X. Gao, C. Peng, et al. "Application of water immersion ultrasonic phased array technology in wheel rim inspection," Advanced Materials Research, vol. 468–471, pp. 733–737, 2022.